RAA 2014 Vol. **14** No. **6**, 648–666 doi: 10.1088/1674–4527/14/6/004
http://www.raa-journal.org *http://www.iop.org/journals/raa*

***R**esearch in*
***A**stronomy and*
***A**strophysics*

The density and temperature dependence of the cooling timescale for fragmentation of self-gravitating disks

Kazem Faghei

School of Physics, Damghan University, Damghan 36715-364, Iran; *kfaghei@du.ac.ir*

Received 2013 April 16; accepted 2014 February 7

Abstract The purpose of this paper is to explore the influences of cooling timescale on fragmentation of self-gravitating protoplanetary disks. We assume the cooling timescale, expressed in terms of the dynamical timescale $\Omega\, t_{\rm cool}$, has a power-law dependence on temperature and density, $\Omega\, t_{\rm cool} \propto \Sigma^{-a} T^{-b}$, where a and b are constants. We use this cooling timescale in a simple prescription for the cooling rate, $du/dt = -u/t_{\rm cool}$, where u is the internal energy. We perform our simulations using the smoothed particle hydrodynamics method. The simulations demonstrate that the disk is very sensitive to the cooling timescale, which depends on density and temperature. Under such a cooling timescale, the disk becomes gravitationally unstable and clumps form in the disk. This property even occurs for cooling timescales which are much longer than the critical cooling timescale, $\Omega\, t_{\rm cool} \gtrsim 7$. We show that by adding the dependence of a cooling timescale on temperature and density, the number of clumps increases and the clumps can also form at smaller radii. The simulations imply that the sensitivity of a cooling timescale to density is more than to temperature, because even for a small dependence of the cooling timescale on density, clumps can still form in the disk. However, when the cooling timescale has a large dependence on temperature, clumps form in the disk. We also consider the effects of artificial viscosity parameters on fragmentation conditions. This consideration is performed in two cases, where $\Omega\, t_{\rm cool}$ is a constant and $\Omega\, t_{\rm cool}$ is a function of density and temperature. The simulations consider both cases, and results show the artificial viscosity parameters have rather similar effects. For example, using too small of values for linear and quadratic terms in artificial viscosity can suppress the gravitational instability and consequently the efficiency of the clump formation process decreases. This property is consistent with recent simulations of self-gravitating disks. We perform simulations with and without the Balsara form of artificial viscosity. We find that in the cooling and self-gravitating disks without the Balsara switch, the clumps can form more easily than those with the Balsara switch. Moreover, in both cases where the Balsara switch is present or absent, the simulations show that the cooling timescale strongly depends on density and temperature.

Key words: accretion, accretion disks — planetary systems: protoplanetary disks — planetary systems: formation

1 INTRODUCTION

Self-gravitating accretion disks can be observed in different contexts over a wide range of sizes, from the large scale of active galactic nuclei (Greenhill & Gwinn 1997; Lodato & Bertin 2003; Kondratko et al. 2005; Lodato 2007) to the small scale of protostellar and protoplanetary disks (Larson 1984; Lin & Pringle 1987; Beltrán et al. 2004; Chini et al. 2004; Rodríguez et al. 2005; Lodato 2007). In this paper, we focus on self-gravitating protoplanetary disks. In such disks, the central object is a young protostar, on which matter from the surrounding disk accretes. Protoplanetary disks are also interesting objects because planets form inside them.

Planets can form through formation of fragments/clumps in a disk. The formation of fragments/clumps in a self-gravitating protoplanetary disk depends on satisfying two conditions. The first condition requires that the disk becomes gravitationally unstable. The stability parameter (Toomre 1964) is

$$Q = \frac{c_{\rm s}\kappa_{\rm ep}}{\pi G\Sigma} ,$$

where $c_{\rm s}$ is the speed of sound in the disk, $\kappa_{\rm ep}$ is the epicyclic frequency, which for a Keplerian disk becomes approximately equal to the angular velocity, G is the gravitational constant and Σ is the surface density. The disk is gravitationally unstable if the Toomre parameter becomes smaller than its critical value, $Q < Q_{\rm crit}$ (Toomre 1964). The critical value is approximately 1 for axisymmetric instabilities, but it becomes as high as $1.5 - 1.7$ for non-axisymmetric instabilities (Durisen et al. 2007). The second condition requires that in addition to the stability criterion mentioned above, the disk must be cooled at a sufficiently fast rate. If we assume the cooling rate to be (Gammie 2001)

$$\left(\frac{du}{dt}\right)_{\rm cool} = -\frac{u}{t_{\rm cool}} ,$$

where u is the internal energy and $t_{\rm cool}$ is the cooling timescale, Gammie (2001) using a local model showed that fragmentation occurs if and only if $\Omega\, t_{\rm cool} \lesssim \beta_{\rm crit}$, where Ω is the angular velocity of the disk or the inverse of dynamical timescale and the critical cooling timescale, $\beta_{\rm crit}$, is approximately 3 for a ratio of specific heats $\gamma = 2$.

The critical cooling timescale has attracted more attention recently in numerous publications (Rice et al. 2003, 2005; Cossins et al. 2010; Meru & Bate 2011a,b; Faghei 2012, 2013; Meru & Bate 2012). For T Tauri disks, Rice et al. (2003) found that the fragments can form for a cooling timescale close to $t_{\rm cool} = 3\Omega^{-1}$. Moreover, they implied that the fragmentation occurs for a longer cooling timescale if the disk is sufficiently massive, which occurs during the earlier stage of the star formation process. Rice et al. (2005) investigated the importance of the equation of state on the fragmentation conditions. They showed the critical cooling timescale increases by decreasing the specific heat ratio (γ). They explained this property as a result of there being a maximum stress that can be maintained by a self-gravitating disk which is in quasi-equilibrium. Cossins et al. (2010), through using a simulation based on smoothed particle hydrodynamics (SPH), studied the stability of self-gravitating protoplanetary disks fragmenting into bound objects. They showed that $\Omega\, t_{\rm cool}$ has a strong dependence on the local temperature. They found that in a self-gravitating disk in which the cooling timescale is not dependent on temperature, a very large accretion rate of $10^{-3}\ M_\odot\ {\rm yr}^{-1}$ is required for fragmentation in the inner radii of the disk, but this is reduced to $10^{-4}\ M_\odot\ {\rm yr}^{-1}$ with a cooling timescale that is dependent on temperature. Meru & Bate (2011a) mentioned that the critical cooling timescale found in previous simulations is only applicable to certain disk surface mass density profiles and for particular disk radii and is not a general rule for all disks. They also found an empirical fragmentation criterion between the cooling timescale in units of the orbital timescale, the surface mass density, the star mass and the radius. Meru & Bate (2011b) performed three-dimensional SPH simulations of disks to investigate the dependence of the critical cooling timescale on resolution. They showed that the critical cooling timescale for fragmentation increases when resolution increases. Meru & Bate (2012) carried out simulations of gravitationally unstable disks using an SPH code and a grid-based hydrodynamics code, FARGO[1] (Masset 2000), to understand their previous non-convergent results (Meru & Bate 2011a). They showed that the convergence of the critical cooling timescale for fragmentation strongly depends on the numerical viscosity which is applied in the simulations of SPH and FARGO. For a certain resolution, the critical cooling timescale increases when the numerical viscosity reduces the dissipation. In SPH simulations, they found that the influence of numerical viscosity on the dissipation is more significant than had previously been expected. They mentioned that, although the quadratic term in the SPH artificial viscosity ($\beta_{\rm sph}$) has very small effects on the dissipation of a gravitationally unstable disk, it can be an important parameter for disk fragmentation.

Faghei (2013) investigated the effects of the cooling function in formation of clumps in protoplanetary disks through the use of two-dimensional SPH simulations. He assumed the ratio of local cooling to dynamical timescales to be a constant and also a function of the local temperature. He found that for a constant β and $\gamma = 5/3$, fragmentation only occurs for $\beta \lesssim 7$. However, in the case of temperature-dependent β and $\gamma = 5/3$, the fragmentation can also occur for larger values of β. Moreover, he found that by increasing the temperature dependence of cooling timescale, the mass accretion rate decreases, the population of clumps/fragments increases, and the clumps/fragments can also form at smaller radii. In recent studies of cooling protoplanetary disks, the cooling timescale expressed in terms of dynamical timescale is assumed to only be a function of temperature and its dependence on density has been ignored (Cossins et al. 2010; Faghei 2012, 2013). Thus, in the present paper, we are going to investigate how cooling timescale is dependent on density and also dependent on both density and temperature in the fragmentation of protoplanetary disks. We will show that the density has a strong effect on the critical cooling timescale, even more than temperature. As mentioned here, Meru & Bate (2012) implied that the artificial viscosity parameters are important for the fragmentation conditions. Thus, we will also consider the influences of these parameters on the simulations which have a cooling timescale that is dependent on temperature and density.

In Section 2, we will outline the numerical techniques used to produce simulations and the key physics related to this work. In Section 3, we outline and discuss the results of the simulations, and we summarize the work in Section 4.

2 SIMULATION METHOD AND RELATED PHYSICS

2.1 Basic Formalism

Two main techniques which are used to study astrophysical fluid dynamics are grid-based modeling and SPH. In grid-based simulations, the spatial domain is divided into grid cells and the equations of hydrodynamics at cell interfaces are calculated. Grid-based methods are well established in hydrodynamic simulations, and have a good pedigree in simulating astrophysical fluids.

SPH usually applies to very dynamical problems which involve high density contrasts, for example the gravitational collapse and fragmentation of molecular clouds. The SPH method was developed by Lucy (1977) and Gingold & Monaghan (1977). SPH can be expressed as a gridless, Lagrangian particle method which is usually used for simulations of self-gravitating astrophysical systems. SPH is closely related to N-body codes in that both are codes based on interactions of particles. Although both methods consider long-range gravity forces, the SPH method also considers pressure and viscosity. In the particle based codes, variables are computed at a particular spatial point. However, each particle in an SPH code represents a volume of fluid with variables that are representative of the surrounding region, such as temperature, density, pressure, etc.

[1] Fast Advection in Rotating Gaseous Objects (FARGO)

In this paper, we implement a Lagrangian hydrodynamical approach through using the two-dimensional capability of the SPH code VINE[2] (Nelson et al. 2009; Wetzstein et al. 2009). In the following, we present some formulations incorporated in VINE, and will discuss some changes we made to the code.

As mentioned, SPH solves the hydrodynamical equations in Lagrangian form and can be regarded as an interpolation technique: the positions of the SPH particles combined with an interpolation kernel W define the fluid quantities throughout the flow. Many kernels can be defined, but we incorporated the widely used kernel that is based on a spline function (Monaghan & Lattanzio 1985)

$$W(r_{ij}, h_{ij}) = \frac{\sigma}{h_{ij}^{\nu}} \begin{cases} 1 - \frac{3}{2}q^2 + \frac{3}{4}q^3 & \text{if } 0 \leq q < 1; \\ \frac{1}{4}(2-q)^3 & \text{if } 1 \leq q < 2; \\ 0 & \text{otherwise}, \end{cases} \tag{1}$$

where i and j denote particles i and j, $r_{ij}[= |\boldsymbol{r}_i - \boldsymbol{r}_j|]$ is the separation between particles i and j, $h_{ij}[= (h_i + h_j)/2]$ is typically defined as the average smoothing length for particles, $q[= r_{ij}/h_{ij}]$ is the dimensionless separation, ν is the number of dimensions and σ is the normalization with values of $2/3$, $10/(7\pi)$ and $1/\pi$ in one, two and three dimensions, respectively. The contribution that particle j, located at $\boldsymbol{r}_j$, makes to the density at location $\boldsymbol{r}_i$ becomes

$$\rho_j(\boldsymbol{r}_i) = m_j W(|\boldsymbol{r}_i - \boldsymbol{r}_j|; h_{ij}), \tag{2}$$

where m_j is mass associated with particle j. The density at $\boldsymbol{r}_i$ is then determined by summing over the N particles that contribute to the density at that location

$$\rho_i \equiv \rho(\boldsymbol{r}_i) = \sum_{j=1}^{N} \rho_j(\boldsymbol{r}_i). \tag{3}$$

Since SPH uses particles with constant masses, mass is conserved trivially and the continuity equation does not need to be solved explicitly. Ignoring self-gravity, the Lagrangian form of the momentum equation can be written as (Benz 1990; Monaghan 1992)

$$\frac{d\boldsymbol{v}_i}{dt} = -\sum_j m_j \left(\frac{p_j}{\rho_j^2} + \frac{p_i}{\rho_i^2} + \Pi_{ij} \right) \nabla_i W_{ij}, \tag{4}$$

where p is the gas pressure, Π_{ij} is the viscous pressure, the sum is over all the neighbors (j) of particle i and $\nabla_i W_{ij}[= \nabla_i W(|\boldsymbol{r}_i - \boldsymbol{r}_j|; h_{ij})]$ is the gradient of the kernel at the location of particle i. In the simulations, we allow the disk to heat up due to both $p\,dV$ work and viscous dissipation. Thus, the energy equation can be written as

$$\frac{du}{dt} = -\frac{p}{\rho} \nabla \cdot \boldsymbol{v} + \phi, \tag{5}$$

where u is internal energy, and $\phi[= \tau_{ij}\partial_j v_i]$ is the viscous dissipation, with τ_{ij} being the viscous stress tensor. The energy equation in the SPH formulation which is used in our simulations is (Benz 1990)

$$\frac{du_i}{dt} = \frac{p_i}{\rho_i^2} \sum_j m_j\, \boldsymbol{v}_{ij} \cdot \boldsymbol{\nabla}_i W_{ij} + \frac{1}{2} \sum_j m_j\, \Pi_{ij}\, \boldsymbol{v}_{ij} \cdot \boldsymbol{\nabla}_i W_{ij}, \tag{6}$$

where $\boldsymbol{v}_{ij}[= \boldsymbol{v}_i - \boldsymbol{v}_j]$ is the velocity of particle i with respect to particle j and Π_{ij} is the artificial viscosity which will be discussed below. In the above equation, the first term corresponds to reversible

[2] Very Interesting Name for an Evolution code (VINE)

($p\,dV$) work and the second term including the heating mechanism is due to the viscous pressure. To perform a basic hydrodynamic simulation, SPH needs an equation of state. If the energy equation is included then typically an ideal gas equation of state will be used

$$p_j = (\gamma - 1)\rho_j u_j\,, \tag{7}$$

where γ is the specific heat ratio.

The most common form used for artificial viscosity Π_{ij} is

$$\Pi_{ij} = \begin{cases} \frac{-\alpha_{ij}\, c_{ij}\, \mu_{ij} + \beta_{ij}\, \mu_{ij}^2}{\rho_{ij}} & \boldsymbol{v}_{ij} \cdot \boldsymbol{r}_{ij} \le 0\,, \\ 0 & \boldsymbol{v}_{ij} \cdot \boldsymbol{r}_{ij} > 0\,. \end{cases} \tag{8}$$

This viscosity vanishes when $\boldsymbol{v}_{ij} \cdot \boldsymbol{r}_{ij} > 0$, which is the SPH equivalent of condition $\nabla \cdot \boldsymbol{v} > 0$. In this artificial viscosity, the α term is linear in the velocity differences, which produces a shear and bulk viscosity to eliminate subsonic velocity oscillations and the quadratic term (the β term) is the von Neumann-Richtmyer viscosity which converts kinetic energy to thermal energy and prevents particles from penetrating into shocks (Monaghan & Gingold 1983). The scalar quantities with both indices i and j are the arithmetic mean of quantities defined for each particle to produce symmetry:

$$\begin{aligned} c_{ij} &= \frac{c_i + c_j}{2}, \qquad \rho_{ij} = \frac{\rho_i + \rho_j}{2}, \\ \alpha_{ij} &= \frac{\alpha_i + \alpha_j}{2}, \qquad \beta_{ij} = \frac{\beta_i + \beta_j}{2}\,, \end{aligned}$$

where c_i is the sound speed for particle i and μ_{ij} has the role of the velocity divergence

$$\mu_{ij} = \frac{h_{ij}\boldsymbol{v}_{ij} \cdot \boldsymbol{r}_{ij}}{\boldsymbol{r}_{ij}^2 + \eta^2 h_{ij}^2}\, f_{ij}\,. \tag{9}$$

Here η is approximately $10^{-1} - 10^{-2}$ to prevent singularities, and f_i is the Balsara switch (Balsara 1995)

$$f_i = \frac{|\langle \boldsymbol{\nabla} \cdot \boldsymbol{v}_i \rangle|}{|\langle \boldsymbol{\nabla} \cdot \boldsymbol{v}_i \rangle| + |\langle \boldsymbol{\nabla} \times \boldsymbol{v}_i \rangle| + \eta'}\,, \tag{10}$$

where η' is also included to prevent divergence. In our simulations, we use the mentioned common form of SPH artificial viscosity, Equation (8), with $\alpha_i = \alpha_{\rm sph} = 1.0$ and $\beta_i = \beta_{\rm sph} = 2.0$, plus the Balsara switch.

2.2 Cooling Timescale

To investigate how self-gravitating disks evolve in the presence of cooling, a cooling term must be added to the energy equation. We assume the cooling term in the energy equation is (Gammie 2001)

$$\left(\frac{du}{dt}\right)_{\rm cool} = -\frac{u}{t_{\rm cool}}\,, \tag{11}$$

where, as mentioned, $t_{\rm cool}$ is the cooling timescale. Using this cooling rate in the energy equation, Equation (5) then becomes

$$\frac{du}{dt} = -\frac{p}{\rho}\nabla \cdot \boldsymbol{v} + \phi - \frac{u}{t_{\rm cool}}. \tag{12}$$

Since each particle has an internal energy per unit mass (u_i), the cooling term for each particle can be written as

$$\left(\frac{du_i}{dt}\right)_{\rm cool} = -\frac{u_i}{t_{\rm cool}}\,. \tag{13}$$

This form of cooling has been used in many previous SPH simulations (e.g., Gammie 2001; Rice et al. 2003, 2005; Cossins et al. 2010; Rice et al. 2012). It is typically assumed that the cooling timescale, expressed in terms of the dynamical timescale $t_{\rm dyn} = 1/\Omega$, is a constant and can be parameterized as

$$\Omega\, t_{\rm cool} = \beta\,, \tag{14}$$

such that fragments/clumps occur for $\beta \lesssim \beta_{\rm crit} = 7$ (e.g., Rice et al. 2003, 2005). As mentioned in the introduction, the critical β parameter depends on the resolution used in the simulation and increases as the resolution is increased (Meru & Bate 2011b). Here, the critical value of β is 7 which is related to a particular resolution. In this paper, we use a fixed number of particles in the simulations, $N_{\rm part} = 125\,000$.

As mentioned in the introduction, Cossins et al. (2010) found that the β parameter strongly depends on temperature and a temperature-dependent cooling timescale can be very effective for forming fragments/clumps in self-gravitating disks. Here, we assume the β parameter is also dependent on density and in the next section by using an SPH simulation, we will confirm this prevision. Thus, we propose the β parameter to have the following form

$$\beta \equiv \Omega\, t_{\rm cool} = \beta_0 \left(\frac{\Sigma}{\Sigma_{\rm min}}\right)^{-a} \left(\frac{T}{T_{\rm min}}\right)^{-b}\,, \tag{15}$$

where a and b are constants which will be determined in simulations, β_0 is the β parameter in Gammie's model, and $\Sigma_{\rm min}$ and $T_{\rm min}$ are respectively the minimum values of surface density and temperature in the entire disk. In the simulation, $\Sigma_{\rm min}$ and $T_{\rm min}$ are calculated at every timestep. We do not implement $\Sigma_{\rm min}$ and $T_{\rm min}$ as constants, because we want to be sure they are really the minimums of surface density and temperature in the gas as time passes. For constant values of $\Sigma_{\rm min}$ and $T_{\rm min}$, it is possible that they are not the minimums for the next timesteps and we may have some particles with $\Sigma < \Sigma_{\rm min}$ or $T < T_{\rm min}$. Thus, to prevent this occurrence, we find the minimums of Σ and T at every timestep. The simulations demonstrate that the changes in $\Sigma_{\rm min}$ and $T_{\rm min}$ are small and do not have significant variations. During the simulations, the minimum density is ~ 10 g cm^{-2} and the minimum temperature only changes between a factor of $\sim 1 - 10$ K. However, the density and temperature in the simulations change by a factor of $100 - 1000$. Thus, it can be mentioned that the β parameter is affected by the changes of Σ or T, rather than changes in $\Sigma_{\rm min}$ or $T_{\rm min}$.

Following Cossins et al. (2010), we assume that the cooling timescale depends on temperature with a negative exponent; so we choose positive values for the parameter b. Moreover, Thoul & Weinberg (1995) and Katz et al. (1996) remarked that the cooling timescale decreases as density increases. Thus, in Equation (15), we assume there is a negative exponent for density that implies there are positive values of parameter a. For $a = b = 0$, the above cooling timescale switches to Gammie's model and thus the β parameter becomes a constant, but for $a > 0$ and $b > 0$, β becomes smaller than β_0. On the other hand, through using Equation (15), the hotter and denser particles achieve a higher cooling rate and can cool rapidly. Thus, this prescription of the cooling rate can enhance the growth and saturation of gravitational instability, because it accelerates the balance between external cooling and internal heating provided by the gravitational instability. In other words, the particles in an annulus of the disk have approximately the same angular velocity, but some of them are hot and dense due to coalescing in a clump. In Gammie's model, these particles achieve approximately the same cooling timescale, $t_{\rm cool} = {\rm constant}/\Omega$ but, in the modified prescription of Gammie's model defined by Equation (15), the particles in an annulus with a higher temperature/density can achieve a higher cooling rate.

2.3 Initial Conditions

As mentioned in the previous sections, we use a Lagrangian hydrodynamical code, VINE. We exploit the two-dimensional ability of the VINE code to perform our simulations. In the simulations, we follow Rice et al. (2005) and Faghei (2013). Here, the physical quantities are given in units with values of a typical protostellar disk. Thus, we choose astronomical unit (AU) and the Sun's mass ($M_\odot$) as the units of length and mass, respectively. Thus, the unit of time becomes $\sqrt{\mathrm{AU}^3/GM_\odot}$, which is equal to a year divided by 2π. We setup the disk with 125 000 SPH particles between $R_{\rm in} = 0.25$ and $R_{\rm out} = 25$, which has a star at the center of the disk. If SPH particles move within a radius $R_{\rm acc} = 0.25$, they are accreted on to the central object. The central object and disk have masses of $M_* = 1$ and $M_{\rm disk} = 0.1$, respectively. For the initial surface density and temperature profiles, we choose $\Sigma \propto R^{-1}$ and $T \propto R^{-0.5}$, respectively. The Toomre stability parameter with these profiles for the surface mass density and temperature is not initially constant and decreases with increasing radius. To normalize temperature, we will assume the disk is gravitationally stable at the beginning of the simulation, with a minimum $Q = 2$ at $R = 25$. With the exception of regions which are very close to the star ($r \lesssim 3$ AU), the remaining parts of the disk under the above particle distribution have the required resolution for fragmentation. (For the resolution required to have fragmentation, please see Lodato & Clarke 2011; Meru & Bate 2012.)

3 SIMULATION RESULTS

In this paper, the effects of cooling timescale are assumed to follow several cases:

- β is a constant, $\beta = \beta_0 = \mathrm{constant}$,
- β is a function of density, $\beta = \beta_0(\Sigma/\Sigma_{\rm min})^{-a}$,
- β is a function of temperature, $\beta = \beta_0(T/T_{\rm min})^{-b}$,
- β is a function of density and temperature, $\beta = \beta_0(\Sigma/\Sigma_{\rm min})^{-a}(T/T_{\rm min})^{-b}$.

We also study the influences of the artificial viscosity parameters, $\alpha_{\rm sph}$ and $\beta_{\rm sph}$, on fragmentation conditions. Thus, for the above cases, we perform simulations with several input parameters, such as $\beta_0, a, b, \alpha_{\rm sph}$, and $\beta_{\rm sph}$. The gas is assumed to be purely in the form of molecular hydrogen; hence, we assume $\mu = 2$ for the molecular weight. For all simulations, we also assume $\gamma = 5/3$. In each run, we stop a simulation when clumps form in the disk. In the cases that do not show fragmentation, we run the simulation for at least seven outer rotation periods, because this is a sufficient time for a disk that does not show fragmentation to reach the steady state. A self-gravitating protoplanetary disk will settle into a quasi-steady state when the mass transfer rate is approximately the same at all radii (Rice & Armitage 2009). Despite this, at the end of the simulations that did not show fragmentation, if there was any evidence for fragmentation, they were continued until either these fragments became much denser than the local density, or they sheared away. In what follows, we describe the results from our suite of simulations.

3.1 $\Omega\, t_{\rm cool}$ is a Constant

In Table 1, we present the various setups for the case of constant $\beta[= \Omega\, t_{\rm cool}]$. The simulations imply that in the case of constant β, fragmentation only occurs for $\beta \lesssim 7$, but this threshold depends on the artificial viscosity parameters. For some values of the artificial viscosity parameters, $\alpha_{\rm sph}$ and $\beta_{\rm sph}$, a faster cooling timescale will be needed. For example, for $(\alpha_{\rm sph}, \beta_{\rm sph}) = (0.1, 0.2)$, the critical cooling timescale is $\beta_{\rm crit} \sim 5 - 6$. However, it increases to $\beta_{\rm crit} \sim 7 - 8$ for sets of $(\alpha_{\rm sph}, \beta_{\rm sph}) = (0.1, 2.0)$, $(1.0, 0.2)$ and $(1.0, 2.0)$. Meru & Bate (2012) showed that for a disk with ratio of specific heats $\gamma = 5/3$ and artificial viscosity $\alpha_{\rm sph} = 0.1$ and $\beta_{\rm sph} = 0.2$, the critical value of the cooling timescale in units of the orbital timescale required for fragmentation is $\beta_{\rm crit} \sim 5 - 6$. However, for the case of $\alpha_{\rm sph} = 0.1$ and $\beta_{\rm sph} = 2$, the critical cooling timescale in their simulations increased to $\beta_{\rm crit} \sim 8 - 8.5$. Thus, in the case of parameters with low artificial viscosity, our results are in accord with their simulations, but for the other values of viscosity parameters, there is a slight

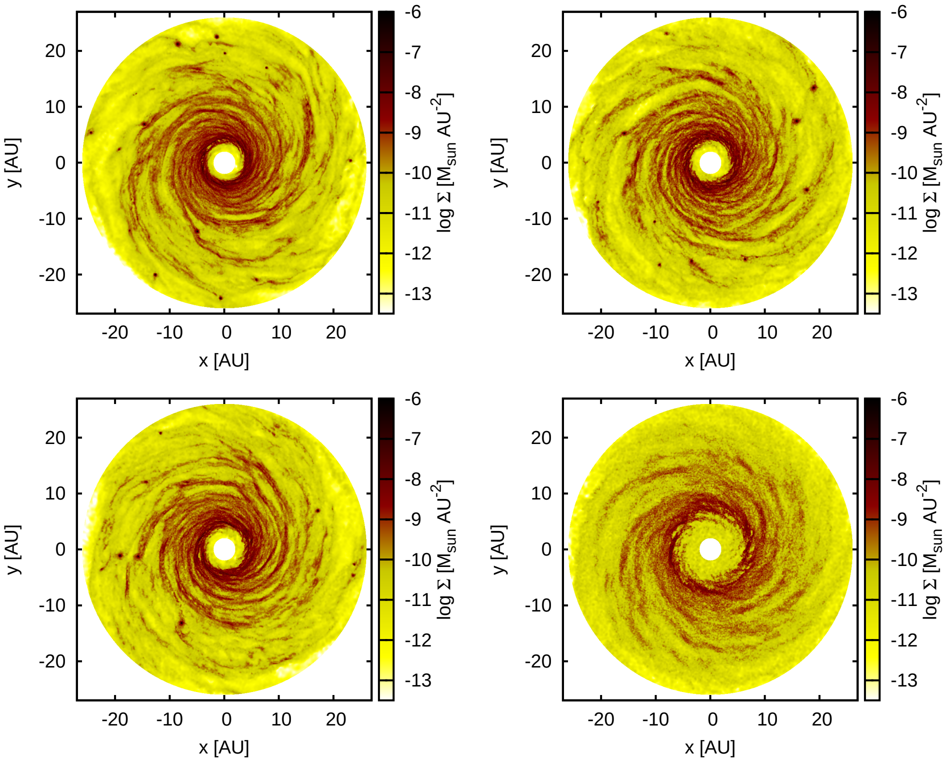

Fig. 1 The logarithm of the surface mass density of the disk at the end of the simulations for $\beta = 6$ and several values of artificial viscosity parameters for simulations Case1-run05 (*top left*), Case1-run06 (*top right*), Case1-run07 (*bottom left*) and Case1-run08 (*bottom right*).

difference. This difference could be due to our 2D simulations compared to their 3D simulations and we also used lower particle numbers, $N_{\rm part} = 125\,000$, in contrast to their $N_{\rm part} = 250\,000$.

Here, we discuss more about the dependence of the critical cooling timescale on the artificial viscosity parameters. In Figure 1, we simulate four disks with several values of the artificial viscosity parameters, i.e. $(\alpha_{\rm sph}, \beta_{\rm sph}) = (1.0, 2.0), (1.0, 0.2), (0.1, 2.0)$ and $(0.1, 0.2)$, which correspond to simulations Case1-run05, Case1-run06, Case1-run07 and Case1-run08, respectively, which are run with the same cooling timescale $\beta = \beta_0 = 6$. As can be seen, except for simulation Case1-run08 in which $(\alpha_{\rm sph}, \beta_{\rm sph}) = (0.1, 0.2)$, clumps form in the other disks. This shows the importance of the artificial viscosity parameters in forming clumps in the cooling and self-gravitating disks. Recently, Meru & Bate (2012) mentioned such a property in self-gravitating disks. They found the artificial viscosity parameters that appear to produce minimum dissipation are $(\alpha_{\rm sph}, \beta_{\rm sph}) = (0.1, 2.0)$.

In Figure 2, we also simulate four disks with the same input parameters as Figure 1, but disks are run with the cooling timescale $\beta = \beta_0 = 7$ for simulations Case1-run09 to Case1-run12. As can be seen, the disk has four clumps in the case $(\alpha_{\rm sph}, \beta_{\rm sph}) = (1.0, 2.0)$, three clumps in the case $(\alpha_{\rm sph}, \beta_{\rm sph}) = (1.0, 0.2)$, one clump in the case $(\alpha_{\rm sph}, \beta_{\rm sph}) = (0.1, 2.0)$ and no clump forms in the case $(\alpha_{\rm sph}, \beta_{\rm sph}) = (0.1, 0.2)$. Although in Figure 1, disks with $(\alpha_{\rm sph}, \beta_{\rm sph}) = (1.0, 0.2)$ and $(\alpha_{\rm sph}, \beta_{\rm sph}) = (0.1, 2.0)$ have approximately similar number of clumps, this property does not occur in Figure 2, as the disk with $(\alpha_{\rm sph}, \beta_{\rm sph}) = (1.0, 0.2)$ has more clumps in contrast with the disk with $(\alpha_{\rm sph}, \beta_{\rm sph}) = (0.1, 2.0)$.

Table 1 List of the main simulations through use of a constant β parameter, $\beta_i = \beta_0 =$ constant. Thus, in these simulations, we have $a = 0$ and $b = 0$.

Simulation name	β_0	$\alpha_{\rm sph}$	$\beta_{\rm sph}$	Clump?
Case1-run01	5	1.0	2.0	yes
Case1-run02	5	0.1	2.0	yes
Case1-run03	5	1.0	0.2	yes
Case1-run04	5	0.1	0.2	yes
Case1-run05	6	1.0	2.0	yes
Case1-run06	6	0.1	2.0	yes
Case1-run07	6	1.0	0.2	yes
Case1-run08	6	0.1	0.2	no
Case1-run09	7	1.0	2.0	yes
Case1-run10	7	0.1	2.0	yes
Case1-run11	7	1.0	0.2	yes
Case1-run12	7	0.1	0.2	no
Case1-run13	8	1.0	2.0	no
Case1-run14	8	0.1	2.0	no
Case1-run15	8	1.0	0.2	no
Case1-run16	8	0.1	0.2	no

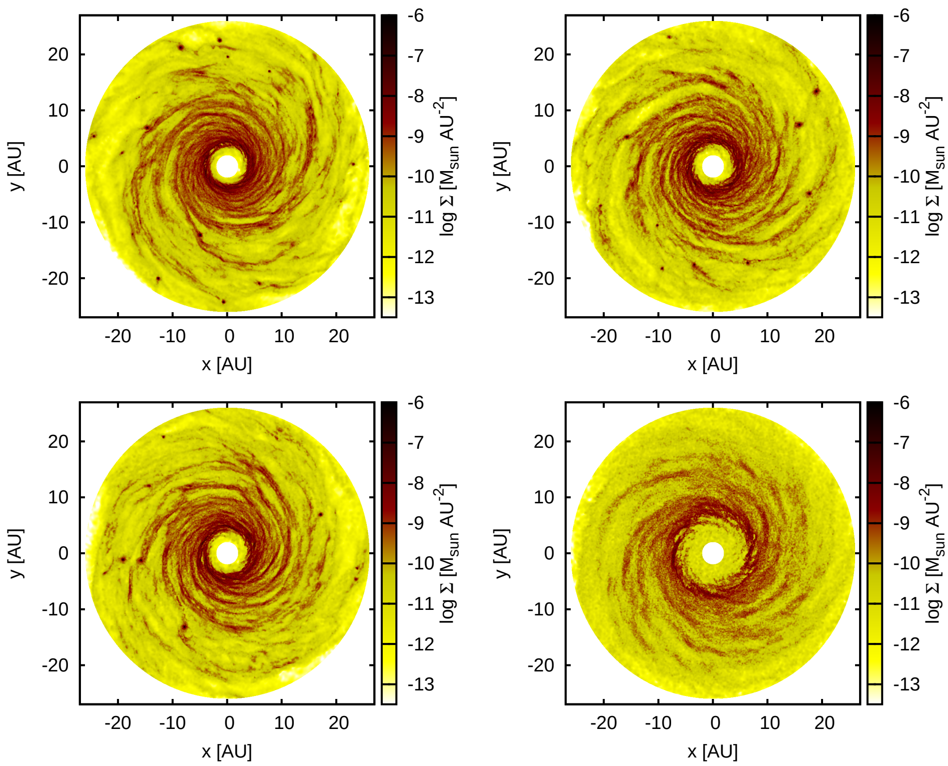

Fig. 2 The logarithm of the surface mass density of the disk at the end of the simulations for $\beta = 7$ and several values of the artificial viscosity parameters for simulations Case1-run09 (*top left*), Case1-run10 (*top right*), Case1-run11 (*bottom left*) and Case1-run12 (*bottom right*).

Figures 1 and 2 demonstrate that most clumps form in the disk with $(\alpha_{\rm sph}, \beta_{\rm sph}) = (1.0, 2.0)$. This means both artificial viscosity parameters are important for the disk with the constant β. Thus, in the current model, we found the linear term in the artificial viscosity can also be important and the clump can form more easily for $(\alpha_{\rm sph}, \beta_{\rm sph}) = (1.0, 2.0)$ in contrast to other chosen values of artificial viscosity parameters in this paper.

3.2 $\Omega\, t_{\rm cool}$ is a Function of Density and Temperature

As seen in the previous section, a self-gravitating disk, which is heated due to gravitational instability and viscous dissipation, will fragment if the cooling timescale is short enough ($\beta \lesssim 7$). Faghei (2013) showed the occurrence of clump formation increases for the cooling timescale that is dependent on temperature, $\beta = \beta_0 (T/T_{\rm min})^{-b}$, with b being a free parameter. Moreover, he showed that clump formation can occur even for cooling timescales longer than the critical cooling timescale.

In Table 2, we have shown some simulations with temperature-dependent cooling timescale, which are simulations Case2-run02, Case2-run5, Case2-run6, Case2-run7 and Case2-run11. These simulations demonstrate that clumps can form even for $\beta_0 \geq 8$.

As mentioned in the introduction, the purpose of this paper is to show that a cooling timescale that is dependent on density is effective for forming clumps in self-gravitating disks. In this way, we will show that fragments can form in a gravitationally unstable disk even if the cooling timescale is not short enough, where $\beta_0 \geq 8$. We investigate this property with a density-dependent cooling timescale, $\beta = \beta_0 (\Sigma/\Sigma_{\rm min})^{-a}$.

In Table 2, we present a disk with this cooling timescale, which applies to simulations Case2-run03, Case2-run08, Case2-run09, Case2-run12, and Case2-run14 to Case2-run17. In these simulations with $\beta_0 \geq 8$, none of the disks were expected to fragment (please see Table 1). As seen in the simulation Case2-run03 in which $\beta_0 = 8$, the clump forms in the disk with $a = 0.025$. As β_0 increases, the minimum value for parameter a also increases. For example, in the simulation Case2-run17 in which $\beta_0 = 20$, clump formation can occur by using $a = 0.19$. In Table 2, we can compare the cooling timescales of density-dependent and temperature-dependent cases. For a disk with $\beta_0 = 8$, the clump forms if the exponent in the temperature-dependent cooling timescale becomes larger than 0.05; however this threshold exponent in the density-dependent cooling timescale decreases to 0.025. This property also happens for larger β_0, for example if $\beta_0 = 12$, the clump forms if $a = 0.1$ or $b = 0.25$. Thus, we can conclude that the sensitivity of the cooling timescale to density is more than for temperature. This property has not been previously reported by researchers.

In Figure 3, we have plotted four disks, in which the cooling timescale in these disks has several power-law dependences on density, i.e. $a = 0, 0.025, 0.05$ and 0.1. The disks are run with $\beta_0 = 8$ and $b = 0$. In the top left panel of Figure 3, we see a disk with the constant cooling timescale $\beta = \beta_0 = 8$. As we expect, no clump forms in this disk. In the other panels of Figure 3, since we use the density-dependent cooling timescale, the clumps form in the disks. Moreover, the number of clumps increases by adding parameter a. In what follows, we explain why this property happens in the density-dependent cooling timescale.

In Figure 4, we have plotted the physical quantities of four disks which were presented in Figure 3. In Figure 4, the red and black points represent the beginning and end of the simulations, respectively. In the third row of this figure, we can see all four disks at the end of the simulations are gravitationally unstable in the region between $5 \lesssim r \lesssim 25$, because the Toomre parameter Q in this region for these disks is approximately unity. However, this instability cannot result in forming clumps in all disks, because in the disk with $a = 0$ and $\beta_0 = 8$, the cooling timescale cannot reach the threshold value needed for fragmentation, as shown in the first panel of the fourth row. However, for the example in the second panel of the fourth row, in which $a = 0.025$ and $\beta_0 = 8$, the cooling timescale changes as the disk evolves. As can be seen in this panel, the β parameter at the end of the simulation has a value between 7 and 8. This range for cooling timescale is sufficient to form a few

Table 2 List of the main simulations which use a cooling timescale that is dependent on density and temperature, $\beta_i = \beta_0(\Sigma_i/\Sigma_{\min})^{-a}(T_i/T_{\min})^{-b}$. The artificial viscosity parameters in these simulations are set to $(\alpha_{\rm sph}, \beta_{\rm sph}) = (1.0, 2.0)$.

Simulation name	β_0	a	b	Clump?
Case2-run01	8	0	0	no
Case2-run02	8	0	0.05	yes
Case2-run03	8	0.025	0	yes
Case2-run04	8	0.02	0.01	yes
Case2-run05	10	0	0.05	no
Case2-run06	10	0	0.1	no
Case2-run07	10	0	0.2	yes
Case2-run08	10	0.05	0	no
Case2-run09	10	0.075	0	yes
Case2-run10	10	0.05	0.1	yes
Case2-run11	12	0	0.25	yes
Case2-run12	12	0.1	0	yes
Case2-run13	12	0.075	0.1	yes
Case2-run14	14	0.15	0	yes
Case2-run15	16	0.17	0	yes
Case2-run16	18	0.18	0	yes
Case2-run17	20	0.19	0	yes

clumps in the disk; please see the top right panel of Figure 3 and the second panel of the first row in Figure 4. For a sufficiently large value of parameter a, the cooling timescale for the entire disk becomes much smaller than the threshold value and so many clumps can form in the gravitationally unstable disk, even at smaller radii. This is because, according to the last row of Figure 4, by using larger a, the β parameter becomes sufficiently small in the inner radii. Thus, the clump can form in the inner radii due to sufficiently small β. As seen for $a \gtrsim 0.025$ and $\beta_0 = 8.0$, the β parameter changes as the disk evolves. According to Equation (15), in the parts of the disk that achieve excess density due to gravitational instability, $\Sigma > \Sigma_{\rm min}$ or $\Sigma/\Sigma_{\rm min} > 1$, the cooling timescale in units of dynamical timescale becomes smaller than 8.0, because, for $\Sigma/\Sigma_{\rm min} > 1$ and $a > 0.025$, $\beta = 8.0(\Sigma/\Sigma_{\rm min})^{-a} \leq 8.0$. Thus, the cooling timescale decreases below the threshold value for clump formation, $\beta \lesssim 8$. In this region for β, the gravitationally unstable parts of the disk again achieve more density due to the lower cooling timescale and so β decreases to less than its previous value. From Figure 4 for $a = 0.1$, we can see this process continues until the β parameter in some parts becomes approximately 3 or even less than 3. This outcome also happens for a temperature-dependent cooling timescale, in which $a = 0$ and $b > 0$ (please see fig. 3 of Faghei 2013). However, for a temperature-dependent cooling timescale, a higher value for temperature exponent b will be needed if we want to see the same properties as in the density-dependent cooling timescale. This means density varies more than temperature in the gravitationally unstable parts of the disk. The density-dependent cooling timescale needs a smaller value for density exponent a in contrast to the temperature exponent b in the temperature-dependent cooling timescale.

From Figure 3 and the first row of Figure 4, we can see for the parameter $a = 0.025$, the clump forms at $r \sim 20$ AU and by adding parameter a, the number of clumps increases and the clumps also form at smaller radii of $r \sim 10$, which means the occurrence of clump formation at smaller radii increases by adding the dependence of cooling timescale on density. This property can be due to the decrease in parameter β by adding parameter a, because recent research based on the stochastic nature of disk fragmentation indicates that the appearance of clump formation increases for smaller values of β (Paardekooper 2012). The formation of clumps at smaller radii by adding the parameter a can be also explained in the following way. For a specified surface density and star mass, Meru &

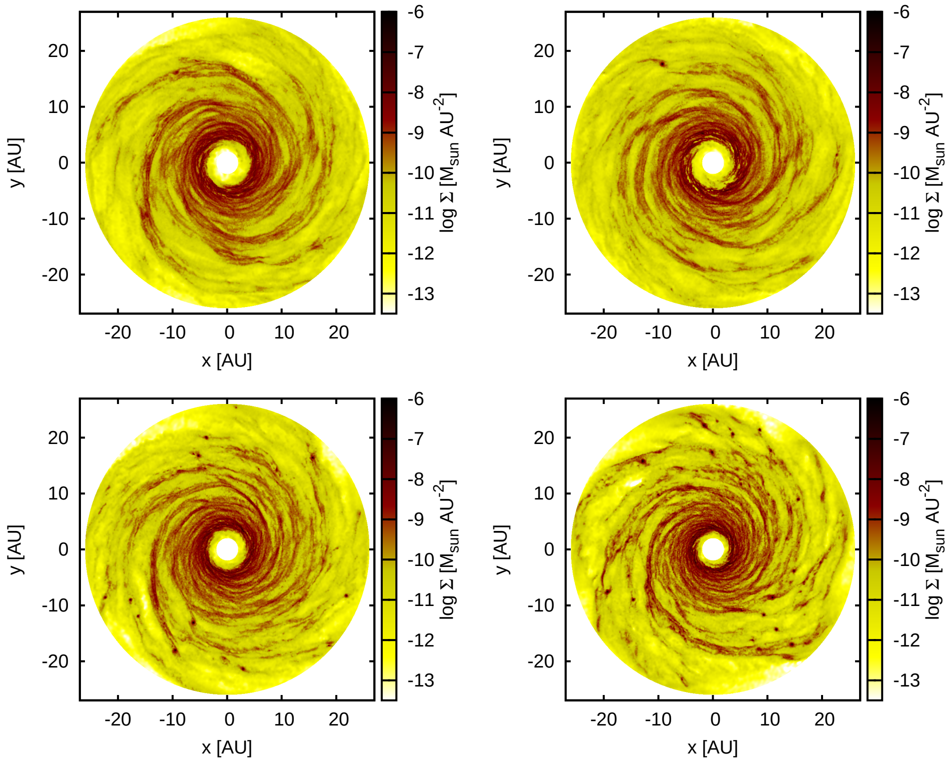

Fig. 3 The logarithmic surface density structure at the end of the simulations for $\beta_0 = 8$, $b = 0$ and $a = 0$ (*top left*), $a = 0.025$, (*top right*), $a = 0.05$ (*bottom left*) and $a = 0.1$ (*bottom right*). The artificial viscosity parameters are set to $\alpha_{\rm sph} = 1.0$ and $\beta_{\rm sph} = 2.0$.

Bate (2011a) showed the radius of the first clumps decreases as the parameter β decreases. In this paper, we use a fixed surface density and star mass, so we expect to decrease the radius where the first clumps form by adding the parameter a, because the parameter β decreases as the parameter a increases.

In the second row of Figure 4, we present the temperature profiles of the disks with $\beta_0 = 8$ and several values for the parameter a. This figure implies that the temperature of the inner region of the disk decreases by adding a. For example, temperature for $r \gtrsim 7.5$ is approximately constant for $a = 0.025$, however, if we use $a = 0.1$, this region extends to smaller radii ($r \gtrsim 5$). In other words, the temperature profile decreases more rapidly by adding the parameter a. This property is due to the decrease in the magnitude of β for inner radii by adding the parameter a, which causes more cooling for inner radii. This property has been previously expressed by Meru & Bate (2011a), in that the temperature profile in a disk with small β will decrease more rapidly than in a disk where β is higher.

We saw the cooling timescales of temperature-dependent or density-dependent cases are effective for forming clumps in the unstable disks. Here, it is interesting to consider whether the cooling timescale that is dependent on temperature and density can be effective in forming clumps.

In Figure 5, we present four disks with a cooling timescale which is dependent on both temperature and density, $\beta = \beta_0(\Sigma/\Sigma_{\rm min})^{-a}(T/T_{\rm min})^{-b}$, for the disks that are run with the same $\beta_0 = 8$. In the top left panel, where $a = b = 0$, as we expect, no clump forms in the disk. This is because the disk has a long constant cooling timescale, $\beta = \beta_0 = 8$. In the other disks, we used the same

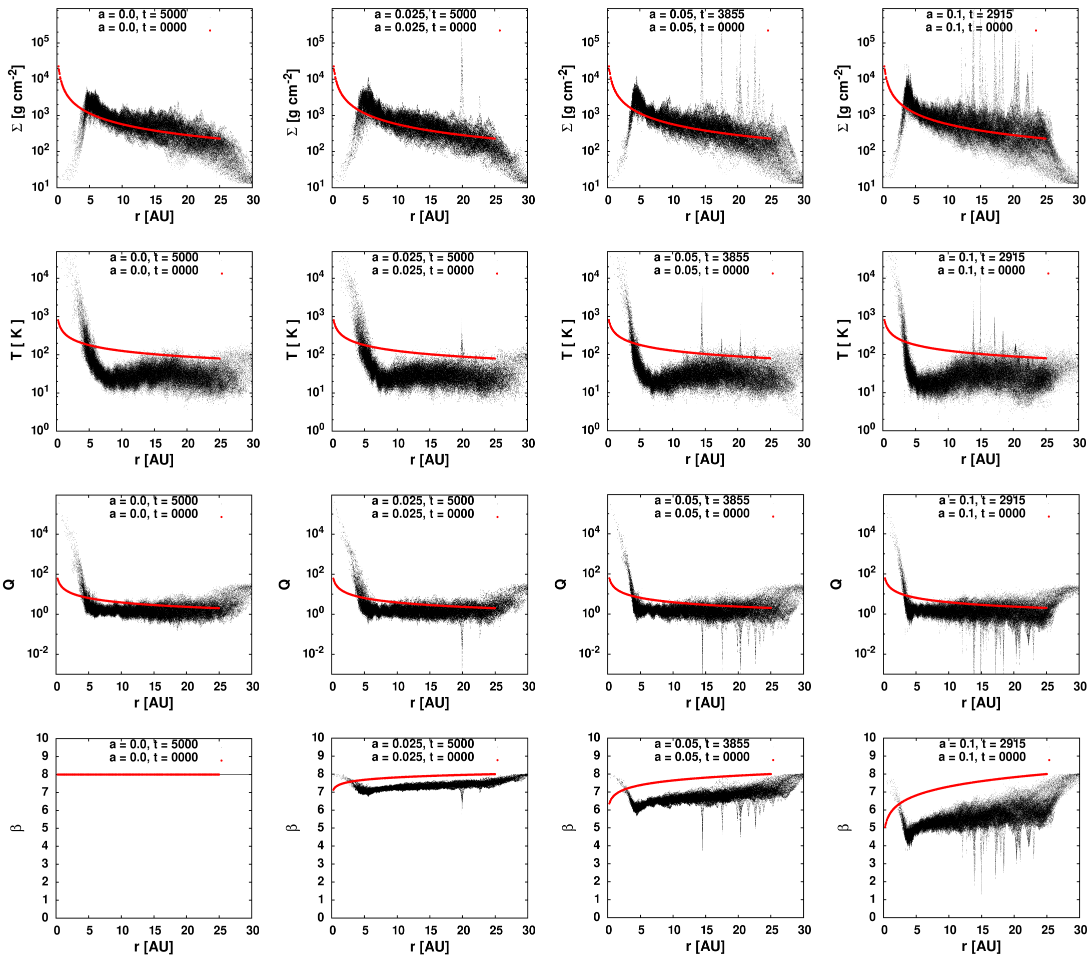

Fig. 4 Physical quantities as functions of radius at the beginning and end of the simulations. The input parameters are $\beta_0 = 8.0$, $b = 0$ and $a = 0.0, 0.025, 0.05$ and 0.1. The artificial viscosity parameters are set to $\alpha_{\rm sph} = 1.0$ and $\beta_{\rm sph} = 2.0$.

$a = 0.01$, but with several values for the parameter b, i.e. $b = 0.02, 0.05$ and 0.1. As can be seen, the number of clumps increases by increasing the parameter b. In Table 2, the simulation Case2-run3 with $\beta_0 = 8$ implies that the minimum value for the parameter a in the density-dependent cooling timescale is 0.025. Moreover, the simulation Case2-run2 implies that for a disk with a temperature-dependent cooling timescale and $\beta_0 = 8$, the minimum value for parameter b to form a clump is 0.05. If we use a cooling timescale which is dependent on both temperature and density, the minimum values which are needed to form a clump are $a = 0.02$ and 0.01. This property also happens even for $\beta_0 > 8$, e.g. simulations Case2-run10 and Case2-run13. Thus, we conclude that the formation of clumps in the disks is enhanced through using a cooling timescale that is dependent on both temperature and density.

Faghei (2013) did not consider the influences of artificial viscosity on his results. In Table 3, similar to the constant cooling timescale, we study the effects of artificial viscosity parameters on a temperature-dependent cooling timescale. We apply several values for artificial viscosity parameters, $(\alpha_{\rm sph}, \beta_{\rm sph}) = (1.0, 2.0), (0.1, 2.0), (1.0, 0.2)$ and $(0.1, 0.2)$, which correspond to simulations

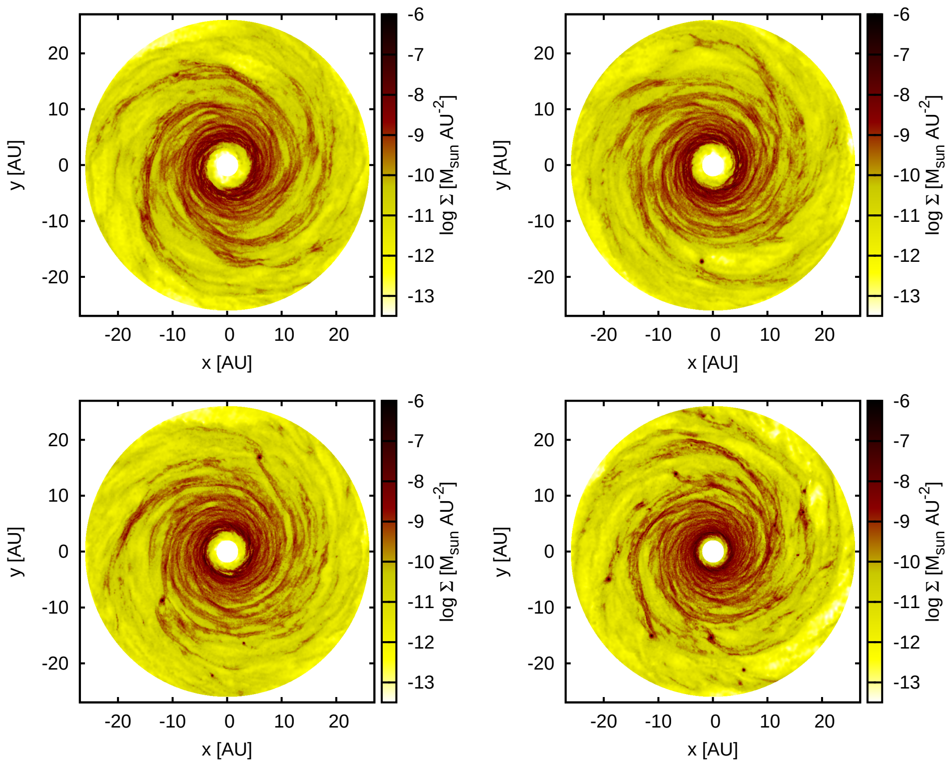

Fig. 5 The logarithmic surface density structure at the end of the simulations for $\beta_0 = 8$, and $a = b = 0$ (*top left*), $a = 0.01$ and $b = 0.02$ (*top right*), $a = 0.01$ and $b = 0.05$ (*bottom left*), and $a = 0.01$ and $b = 0.1$ (*bottom right*). The artificial viscosity parameters are set to $\alpha_{\rm sph} = 1.0$ and $\beta_{\rm sph} = 2.0$.

Case3-run05 to Case3-run8, respectively. In these simulations, we applied $\beta_0 = 8.0$. Fragmentation occurs in simulations Case3-run05 and Case3-run07, in which $\beta_{\rm sph} = 2$. However, no sign of clump formation appears for simulations Case3-run06 and Case3-run08, in which $\beta_{\rm sph} = 0.2$. Meru & Bate (2012) explained this property by the quadratic term in artificial viscosity. They mentioned that the dissipation increases for very small values of the quadratic term in artificial viscosity. Moreover, they explained this property in the following way. Because of the presence of shocks, the velocity dispersion of random particles increases, so the dissipation significantly deviates from the continuum limit in SPH equations.

In Table 3, in simulations Case3-run09 to Case3-run12 and Case3-run17 to Case3-run20, we investigate the influences of the artificial viscosity parameters on the density-dependent cooling timescale. We have also considered this for the simulations Case3-run13 to Case3-run16 and Case3-run21 to Case3-run23, in which the cooling timescale is dependent on density and temperature. As can be seen, in all cases with $(\alpha_{\rm sph}, \beta_{\rm sph}) = (0.1, 0.2)$, no clump forms in the disks. In the cases for which $(\alpha_{\rm sph}, \beta_{\rm sph}) = (0.1, 2.0)$ and $(\alpha_{\rm sph}, \beta_{\rm sph}) = (1.0, 0.2)$, a clump can form in the disks. We found the clump can more easily form for $(\alpha_{\rm sph}, \beta_{\rm sph}) = (1.0, 2.0)$ in contrast to other chosen values of artificial viscosity parameter used in this paper. This property also happened for the constant β.

Here, we try to discuss more about the effects of the artificial viscosity parameters on the β parameter.

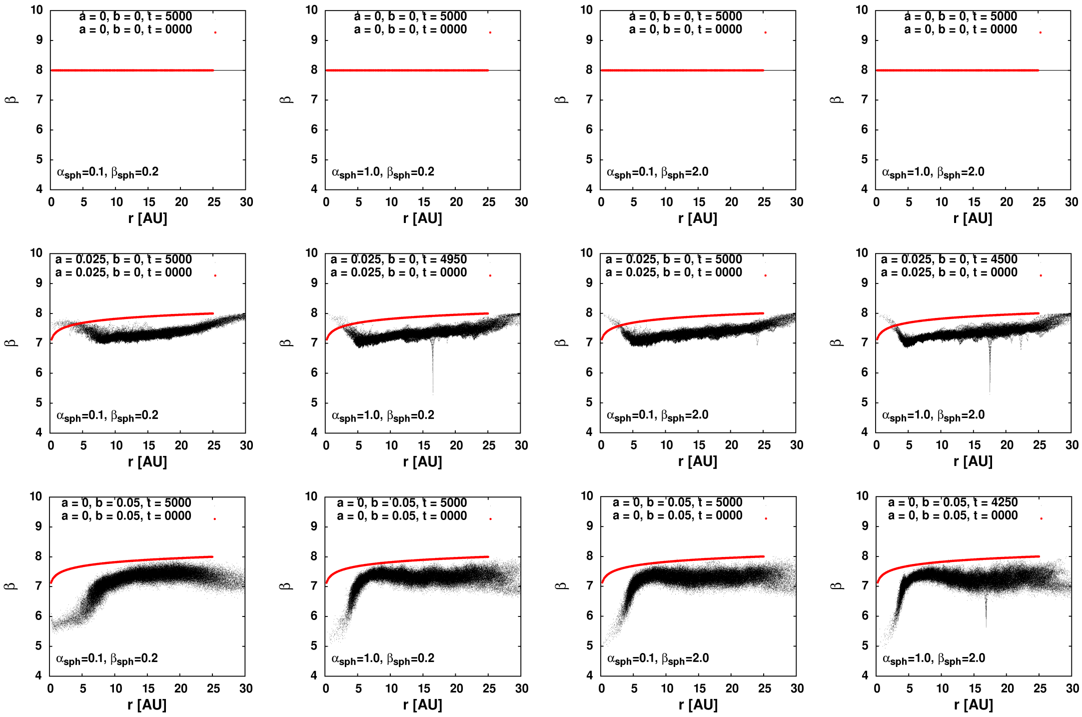

Fig. 6 The ratio of cooling to dynamical timescales $\Omega\, t_{\rm cool}$ at the beginning and end of the simulations for $\beta_0 = 8.0$.

In Figure 6, the β parameter has been considered for $\beta_0 = 8.0$ with several values of the artificial viscosity parameters, $(\alpha_{\rm sph}, \beta_{\rm sph}) = (1.0, 2.0)$, $(0.1, 2.0)$, $(1.0, 0.2)$ and $(0.1, 0.2)$. In the first row of Figure 6, the β parameter is constant and so cannot be changed by the artificial viscosity parameters. It causes all parts of the disk to have a long cooling timescale, $\beta = \beta_0 = 8$, and so no clump forms in the disk for simulations Case3-run01 to Case3-run04. In the second row, we consider a density-dependent cooling timescale, $a = 0.025$ and $b = 0$. For such input parameters, which are dependent on values of the artificial viscosity parameters, the clumps can form in the disk. For $(\alpha_{\rm sph}, \beta_{\rm sph}) = (0.1, 0.2)$, the β parameter is above the critical value for fragmentation, $\beta > \beta_{\rm crit} = 7.0 - 8.0$. Thus, as we expect, no clump forms in the disk for simulation Case3-run12. However, for the other values of the viscosity parameters, the β parameter in a few parts of the disk becomes lower than $\beta_{\rm crit}$. Thus, the clumps form in these places for simulations Case3-run09 to Case3-run11. In the last row of Figure 6, a similar property happens for a cooling timescale that is dependent on density and temperature, in which $a = 0.02$ and $b = 0.01$. As can be seen in the first panel of Figure 6, the β parameter in all parts is larger than the critical value and the clump cannot form in the disk for simulation Case3-run16. However, for the other viscosity parameters, the β parameter in a few parts of the disk becomes low enough that a clump forms in the disk for simulations Case3-run13 to Case3-run15.

Balsara (1995) suggested adding a shear correction term, known as the Balsara switch, to the standard SPH artificial viscosity which maintains viscosity in compressional flows but reduces it to zero in pure shear flows. For all the simulations presented until now, we have used the Balsara form of the artificial viscosity. Now, it will be interesting to see what will happen to the fragmentation condition due to the absence of the Balsara switch in the artificial viscosity.

Table 3 List of the main simulations that use a density- and temperature-dependent cooling timescale, $\beta_i = \beta_0(\Sigma_i/\Sigma_{\min})^{-a}(T_i/T_{\min})^{-b}$. In these simulations, we investigate the influences of the artificial viscosity parameters on the fragmentation condition.

Simulation name	β_0	a	b	$\alpha_{\rm sph}$	$\beta_{\rm sph}$	Clump?
Case3-run01	8	0	0	1.0	2.0	no
Case3-run02	8	0	0	0.1	2.0	no
Case3-run03	8	0	0	1.0	0.2	no
Case3-run04	8	0	0	0.1	0.2	no
Case3-run05	8	0	0.05	1.0	2.0	yes
Case3-run06	8	0	0.05	0.1	2.0	yes
Case3-run07	8	0	0.05	1.0	0.2	no
Case3-run08	8	0	0.05	0.1	0.2	no
Case3-run09	8	0.025	0	1.0	2.0	yes
Case3-run10	8	0.025	0	0.1	2.0	yes
Case3-run11	8	0.025	0	1.0	0.2	yes
Case3-run12	8	0.025	0	0.1	0.2	no
Case3-run13	8	0.02	0.01	1.0	2.0	yes
Case3-run14	8	0.02	0.01	0.1	2.0	yes
Case3-run15	8	0.02	0.01	1.0	0.2	yes
Case3-run16	8	0.02	0.01	0.1	0.2	no
Case3-run17	10	0.075	0	1.0	2.0	yes
Case3-run18	10	0.075	0	0.1	2.0	no
Case3-run19	10	0.075	0	1.0	0.2	yes
Case3-run20	10	0.075	0	0.1	0.2	no
Case3-run21	10	0.05	0.1	1.0	2.0	yes
Case3-run22	10	0.05	0.1	1.0	0.2	yes
Case3-run23	10	0.05	0.1	0.1	2.0	yes

In Table 4, we have performed a few simulations to investigate this issue. Here, we assume the β parameter to be a constant and also assume the β parameter to be dependent on density and temperature. In the case of constant β parameter, the critical β parameter is 7.0 if we use the Balsara switch for simulation Case4-run01. However, the critical β parameter will be 8.0 without using the Balsara switch for simulation Case4-run02. It means the critical cooling timescale becomes longer without the use of the Balsara switch. For the density-dependent cooling timescale and using the Balsara switch, the critical values of a for $\beta_0 = 8.0$ and 10.0 respectively are $a = 0.025$ and 0.075 for simulations Case4-run05 and Case4-run10. However, without the use of the Balsara switch, the critical values of a decrease to $a = 0.0$ and 0.05 for simulations Case4-run04 and Case4-run11. In the simulations Case4-run06 and Case4-run12, we use the Balsara switch and the cooling timescale is dependent on temperature. The critical values of b in these simulations, in which $\beta_0 = 8.0$ and 10.0, respectively become 0.05 and 0.2. However, these critical values decrease to 0.0 and 0.125 without the use of the Balsara switch for simulations Case4-run04 and Case4-run13. For a β parameter that is dependent on both density and temperature, a similar property appears and the critical exponents decrease without the use of the Balsara switch for simulation Case4-run17.

Here, we can conclude that in the cases of constant and non-constant β parameter, the occurrence of disk fragmentation increases if we do not use the Balsara switch. This property can be explained in the following way. Here, since the Balsara switch reduces the heating rate due to viscosity, we expect to more easily form fragments, but such a result did not occur, because, in the absence of the Balsara switch, the viscous dissipation increases and so temperature of the flow also increases. Since the cooling rate has an explicit linear dependence on temperature, $(du/dt)_{\rm cool} \propto u \propto T$, it also increases in the absence of the Balsara switch. As the simulations indicate, the differences between heating and cooling rates in the presence or absence of the Balsara switch are approximately the same.

Table 4 List of the main simulations that use a density and temperature dependent cooling timescale, $\beta_i = \beta_0(\Sigma_i/\Sigma_{\min})^{-a}(T_i/T_{\min})^{-b}$. In these simulations, we investigate the influences of the presence/absence of the Balsara switch on the fragmentation condition. The artificial viscosity parameters are set to $\alpha_{\rm sph} = 1.0$ and $\beta_{\rm sph} = 2.0$.

Simulation name	β_0	a	b	Balsara switch	Clump?
Case4-run01	7	0	0	yes	yes
Case4-run02	7	0	0	no	yes
Case4-run03	8	0	0	yes	no
Case4-run04	8	0	0	no	yes
Case4-run05	8	0.025	0	yes	yes
Case4-run06	8	0	0.05	yes	yes
Case4-run07	10	0	0	yes	no
Case4-run08	10	0	0	no	no
Case4-run09	10	0.05	0	yes	no
Case4-run10	10	0.075	0	yes	yes
Case4-run11	10	0.05	0	no	yes
Case4-run12	10	0	0.2	yes	yes
Case4-run13	10	0	0.125	no	yes
Case4-run14	10	0	0.125	yes	no
Case4-run15	10	0.025	0.075	yes	no
Case4-run16	10	0.05	0.1	yes	yes
Case4-run17	10	0.025	0.075	no	yes

The present study also shows that the cooling timescale which is dependent on density and temperature is effective for forming fragments regardless of the presence or absence of the Balsara switch. Moreover, the sensitivity of the cooling timescale to density is more than simply temperature regardless of the presence or absence of the Balsara switch in the simulations.

4 SUMMARY AND DISCUSSION

In this paper, we have simulated cooling and self-gravitating protoplanetary disks using a two-dimensional, smoothed particle hydrodynamics method. We allowed the heating effects in the disk due to work done on the gas and artificial viscosity to capture shocks. The disk was cooled using a simple parameterization for the cooling function (Gammie 2001). Cossins et al. (2010) and Faghei (2013) showed a cooling timescale that is dependent on temperature is effective for forming clumps in the unstable disks. In this paper, we assumed the cooling timescale, expressed in terms of the dynamical timescale, is a function of temperature and also density. For the shearing effects, we exploit a common form of artificial viscosity given by Monaghan & Gingold (1983), which uses the parameters $\alpha_{\rm sph}$ and $\beta_{\rm sph}$. We applied several values for these parameters to investigate their influences on conditions that lead to the formation of fragments. In the SPH simulations, the shear viscosity and dissipation due to viscosity can be included through the use of artificial viscosity. When using a large viscosity, the evolution of the disk becomes artificial, but the simulations of shocks will be inaccurate if we use a very small value for the artificial viscosity (Meru & Bate 2012).

For considering a cooling timescale that is dependent on density and temperature, we have performed the simulations with long cooling timescales, $\beta_0 \gtrsim 8$, to determine whether a clump can form. The simulations showed that the formation of a clump accelerates if we use such a cooling timescale. For example by adding the dependence of the cooling timescale on both density and temperature, the number of clumps increases and the clumps can even form at smaller radii. These properties are in accord with recent research based on the stochastic nature of disk fragmentation, which indicates that the appearance of clumps increases for smaller values of β (Paardekooper 2012). In this research, we also considered the influences of artificial viscosity parameters for such a cooling timescale. We found the reduction in the quadratic term of artificial viscosity from 2.0 to 0.2 can suppress the fragmentation of the disk. This property agrees with simulations by Meru & Bate (2012). In addition, the simulations imply that in some cases where $\beta_{\rm sph} = 0.2$, using $\alpha_{\rm sph} = 1.0$ can compensate the suppression due to the low quadratic term in artificial viscosity. We found that for the chosen values of artificial viscosity parameters, $(\alpha_{\rm sph}, \beta_{\rm sph}) = (1.0, 2.0), (0.1, 2.0), (1.0, 0.2)$ and $(0.1, 0.2)$, a fragment can form more easily in a self-gravitating disk with $(\alpha_{\rm sph}, \beta_{\rm sph}) = (1.0, 2.0)$. In the current work, we generally used the Balsara form of artificial viscosity. Nevertheless, we also performed a few simulations without the Balsara form of artificial viscosity. We found that the occurrence of fragmentation is more for simulations without the Balsara switch in contrast to simulations with the Balsara switch. Moreover, the simulations implied that the critical cooling timescale strongly depends on density and temperature in both cases with the Balsara form of artificial viscosity and without it.

In this paper, the model has some limitations. For example, we have only performed a 2D SPH simulation due to limitations of computational resources. However, the requirement of 3D simulation is fundamental, because the typical size of gravitational disturbances is related to the disk's thickness, so that any simulation with zero thickness will lead to an underestimate of global effects (Lodato & Rice 2005). Thus, the consideration of the present results in a 3D SPH simulation is necessary for future research. In this paper, we studied the cooling timescale which is dependent on density and temperature, and we only used certain profiles for surface mass density and temperature, $\Sigma \propto r^{-1}$ and $T \propto r^{-0.5}$. Since the importance of the surface mass density profile in place of clump formation has been confirmed (Meru & Bate 2011a), the study of the present model through using several surface mass density and temperature profiles is an interesting subject for future research. Here, we applied a simple model for the cooling rate, in which cooling timescale is dependent on density and temperature. This cooling rate may fail for some values of density or temperature. For example, in the regions where clump formation in gas becomes very dense ($\rho \gtrsim 5 \times 10^{-10}\ {\rm g\,cm^{-3}}$), this cooling rate may not be valid, because for values of density larger than this threshold value, the temperature evolves in a nearly adiabatic fashion (Boss 2001; Mayer et al. 2004). Thus, more consideration of this cooling rate compared to a real cooling rate based on the opacity regime is strongly suggested to exactly specify the domain where this simple cooling rate is valid. In the simulations, we only used a fixed mass for the disk. Simulations with several masses for the disks will also be interesting for subsequent works.

Acknowledgements I would like to thank the anonymous reviewer for very carefully reading the paper and very useful comments that helped me improve the initial version of the paper. Financial support from the research council of Damghan University with grant number 91/phys/108/204 is acknowledged.

References

Balsara, D. S. 1995, Journal of Computational Physics, 121, 357

Beltrán, M. T., Cesaroni, R., Neri, R., et al. 2004, ApJ, 601, L187

Benz, W. 1990, in Numerical Modelling of Nonlinear Stellar Pulsations Problems and Prospects, ed. J. R. Buchler , 269 (Dordrecht: Kluwer)

Boss, A. P. 2001, ApJ, 563, 367

Chini, R., Hoffmeister, V., Kimeswenger, S., et al. 2004, Nature, 429, 155

Cossins, P., Lodato, G., & Clarke, C. 2010, MNRAS, 401, 2587

Durisen, R. H., Boss, A. P., Mayer, L., et al. 2007, Protostars and Planets V, eds. B. Reipurth, D. Jewitt, & K. Keil (Tucson: University of Arizona), 607

Faghei, K. 2012, RAA (Research in Astronomy and Astrophysics), 12, 331

Faghei, K. 2013, RAA (Research in Astronomy and Astrophysics), 13, 170

Gammie, C. F. 2001, ApJ, 553, 174
Greenhill, L. J., & Gwinn, C. R. 1997, Ap&SS, 248, 261
Katz, N., Weinberg, D. H., & Hernquist, L. 1996, ApJS, 105, 19
Kondratko, P. T., Greenhill, L. J., & Moran, J. M. 2005, ApJ, 618, 618
Larson, R. B. 1984, MNRAS, 206, 197
Lin, D. N. C., & Pringle, J. E. 1987, MNRAS, 225, 607
Lodato, G. 2007, Nuovo Cimento Rivista Serie, 30, 293
Lodato, G., & Bertin, G. 2003, A&A, 398, 517
Lodato, G., & Rice, W. K. M. 2005, MNRAS, 358, 1489
Lodato, G., & Clarke, C. J. 2011, MNRAS, 413, 2735
Lucy, L. B. 1977, AJ, 82, 1013
Masset, F. 2000, A&AS, 141, 165
Mayer, L., Wadsley, J., Quinn, T., & Stadel, J. 2004, in Astronomical Society of the Pacific Conference Series, 321, Extrasolar Planets: Today and Tomorrow, eds. J. Beaulieu, A. Lecavelier Des Etangs, & C. Terquem, 290
Meru, F., & Bate, M. R. 2011a, MNRAS, 410, 559
Meru, F., & Bate, M. R. 2011b, MNRAS, 411, L1
Meru, F., & Bate, M. R. 2012, MNRAS, 427, 2022
Monaghan, J. J. 1992, ARA&A, 30, 543
Gingold R. A., & Monaghan J. J., 1977, MNRAS, 181, 375
Monaghan, J. J., & Gingold, R. A. 1983, Journal of Computational Physics, 52, 374
Monaghan, J. J., & Lattanzio, J. C. 1985, A&A, 149, 135
Nelson, A. F., Wetzstein, M., & Naab, T. 2009, ApJS, 184, 326
Paardekooper, S.-J. 2012, MNRAS, 421, 3286
Rice, W. K. M., Armitage, P. J., Bate, M. R., & Bonnell, I. A. 2003, MNRAS, 339, 1025
Rice, W. K. M., Lodato, G., & Armitage, P. J. 2005, MNRAS, 364, L56
Rice, W. K. M., & Armitage, P. J. 2009, MNRAS, 396, 2228
Rice, W. K. M., Forgan, D. H., & Armitage, P. J. 2012, MNRAS, 420, 1640
Rodríguez, L. F., Loinard, L., D'Alessio, P., Wilner, D. J., & Ho, P. T. P. 2005, ApJ, 621, L133
Thoul, A. A., & Weinberg, D. H. 1995, ApJ, 442, 480
Toomre, A. 1964, ApJ, 139, 1217
Wetzstein, M., Nelson, A. F., Naab, T., & Burkert, A. 2009, ApJS, 184, 298